

# Channel Optimization Design - A Case study of Shawan River

## Report

Teammates: Pan Xinxin (Leader), Wang Yalin, Zhao Lingzhen, Tang Jiatong

Key words: Frouder number; Stable flow; Tubulence; Sediment transport; Weir shape.

## 1. Introduction

In open channel flood design, there are some critical design principles to meet the co-equal goals of increasing flood protection and ecosystem conservation[1]:

- (1) Increase the average channel width;
- (2) Decrease the average flow depth and velocity to balance between preventing sedimentation and erosion;
- (3) Added submerged trapezoidal weirs to block sand and adjust flow velocity and discharge.

To verify the optimization of channel engineering and the corresponding hydraulic properties, 900m-long Shawan river (Chainage: S3+570.21 ~ S4+470.05) (see in Fig. 1) is taken as a case. Shawan River Watershed belongs to the Pearl River Delta Basin, one of the most critical basins in Shenzhen.

Shawan River optimization project in 2016 took some measures according to the above principles: [2]

- (1) Increased the channel bottom width;
- (2) Rebuilt trapezoidal channel section;
- (3) Added submerged trapezoidal weirs to block sand and adjust flow velocity and discharge.

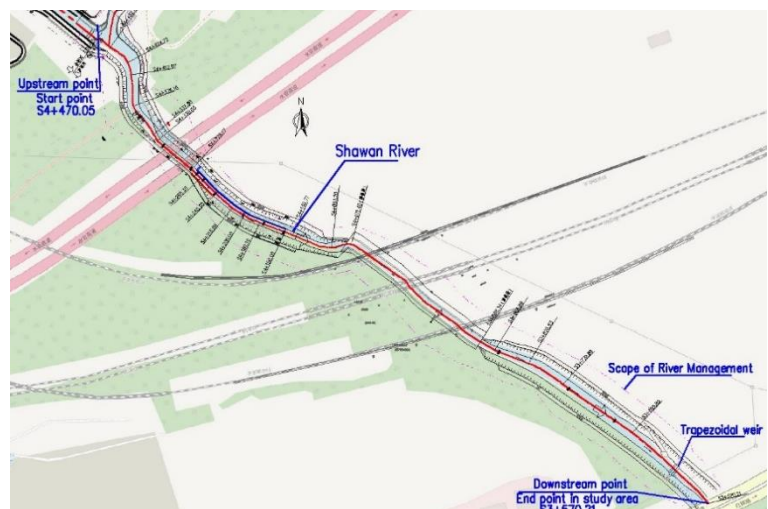


Fig. 1. 900-meter-long upstream in Shawan channel

We discuss and demonstrate these principles focusing on hydraulic properties:

- (1) Flow state in natural and optimization channel;
- (2) The most hydraulically efficient channel sections based on optimization section;
- (3) The suitable upstream slope of weirs with the asymmetry of weir section.



Fig. 2. A long-term averaged flow state in weir

## 2. Methodology

### 2.1. Compute flow in optimization and natural channel

#### 2.1.1. Hydrological Model MIKE

DHI MIKE is one of the most widely used hydrodynamic models. It is used to simulate water surface profiles and discharge in rivers. [3] To simulate a fully dynamic wave description, it solves the equations of conservation of continuity and momentum (the ‘Saint Venant’ equations).

The data required for the MIKE HD module include a topographic map of the study area, river geometry and time series of water level and discharge.

The Q-h relation as boundary condition is suitable for modelling the equilibrium flow.

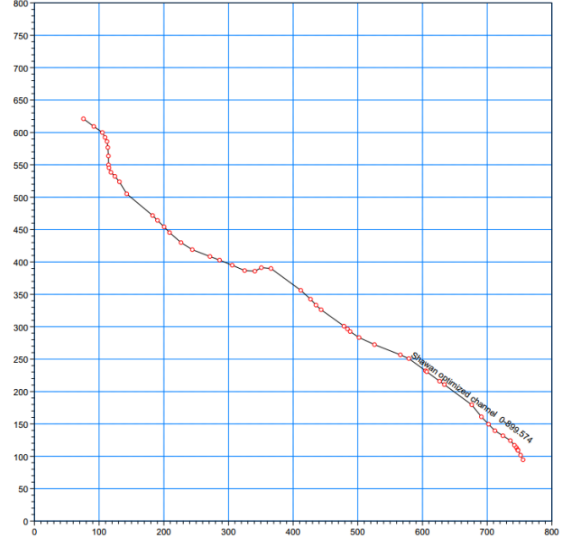


Fig. 3. River network in MIKE

#### 2.1.2. Flow condition and input setup

3 conditions for discussion:

- 1) Natural channel with a extreme discharge  $Q=200m^3/s$  at the upstream from a 100-year return period storm ( $P=1\%$ ), and corresponding to the initial water level at the downstream;
- 2) Optimized channel with the same BC with 1);
- 3) Natural channel with a long-term averaged discharge  $Q=50m^3/s$  at the upstream ( $P=50\%$ ) and its corresponding to the water level.

The river geometry is defined by inserting the river cross-sections with around 50m interval distance along the channel. Considering the different Manning's coefficient  $n$ ,  $n=0.030$  for Natural channel with sand bed, and  $n=0.025$  for Optimized channel with Coir Blanket Lining (see in Fig. 4).

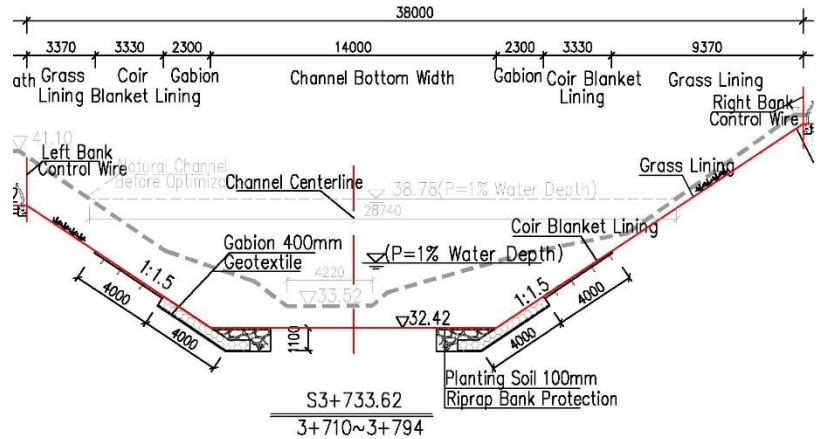


Fig. 4. Optimization channel section

#### 2.1.3. Froude Number

In general, it can be calculated by the following equation:

$$F_r = \frac{V}{\sqrt{gh}} \quad (2-1)$$

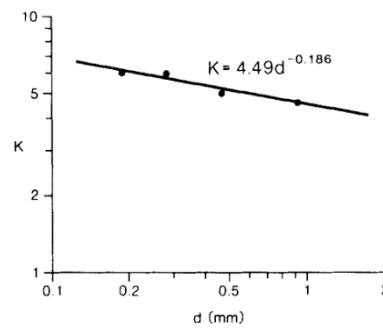
The ideal minimum value of  $Fr$  can be obtained from simulation. The simulation is based on several assumptions: the channel of the sand-bed river is alluvial; the adjustments of slope and cross-sectional form should satisfy the water and sediment transport equilibrium conditions; the adjustments should be associated with resistance of bed form and sediment particles to the flow.

Based on the simulation results,  $Fr$  can be found to have a minimum value, by which a certain set of hydraulic geometry can be identified. For the other elements (e.g. the stream power per unit length (slope) and per unit weight of water, the resistance to flow), the simulations did not find them to have minimum values. It can be used to identify a unique stable equilibrium state. According to the analysis, this  $Fr_{min}$  should represent the equilibrium state of the highest stability[4]. And from the lab test, the regression equations can be got:

$$Fr_{min} = K \times (V \times J)^b \quad (2-2)$$

Where  $b$  is almost constant;  $K$  differs according to the size of sediment;  $J$  is the slope.  $b$  and  $K$  can be considered as constant terms, where  $K$  varies according to the sand and gravel diameter  $d$ . From the lab test, the relation between  $K$  and  $d$  can be obtained (Fig. 5).[4]

$$K = 4.49 \times d^{-0.186} \quad (2-3)$$



So, finally, the formula of  $Fr_{min}$  in this case is obtained:

Fig. 5 The relation of  $K$  to  $d$

$$Fr_{min} = 4.49 \times d^{-0.186} \times (VJ)^b \quad (2-4)$$

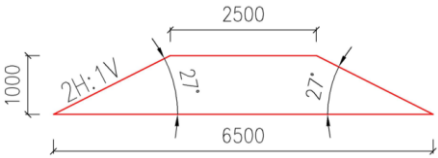
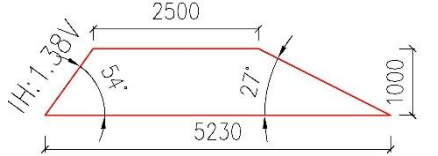
## 2.2. Configuration and Numerical Setup for weirs

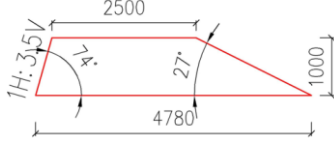
This study is based on numerical simulation and corresponding case comparison.

### 2.2.1. Flow and weir condition

To qualify the asymmetry of weir section leading a more efficient flow, according to the reference weir tested[5], we choose 3 types of the upstream slope ( $\theta$ ) of weir in this project, that are  $27^\circ$ ,  $54^\circ$  and  $74^\circ$ . Besides, the weir height  $Z=1m$ , the weir crest length  $L_{cr}=2.5m$  and the downstream slope  $\theta_d=27^\circ$  are actually optimized design parameters. (See the weir design parameters in Table. 1).

Table. 1. Geometrical conditions of the weir

Weir No.	Weir section	Upstream slope $\theta$	Upstream H:V	Weir Length(m)
1		$27^\circ$	1:0.5	6.50
2		$54^\circ$	1:1.38	5.23

3		74°	1:3.5	4.78
---	---	-----	-------	------

For the simulation channel, the total length is  $30m$ , and set a constant distance  $L_1=10m$  between the upstream weir and the start of the channel. Considering the weir submerged condition, a flow volume of water depth  $H_0=1.5m$  is used to model the boundary condition of  $Q=50m^3/s$  ( $P=50\%$  corresponds to a long-term average water level), and the initial condition of the water depth is equal to  $0.75m$ , that is  $0.25m$  lower than the weir to make the water-surface profile obvious.

For the channel, choose the downstream part with the bottom width equal to  $14m$ .

### 2.2.2. Numerical Setup

FLOW-3D is a computational fluid dynamic code implementing the finite volume method to solve the Reynolds-averaged N-S equations with a VOF method to track the free surface[6].

For a high-effective computational time, adopt the structured and mixed orthogonal mesh: the smaller size for the weir area (cell size= $0.25m$ ) and the bigger size for the upstream and downstream channel (cell size= $0.5m$ ) (See in Fig. 6~9). Therefore, this simulation is implemented in such a way that the number of cells is greater than 60,000 for this computational domain about 30m-long channel.

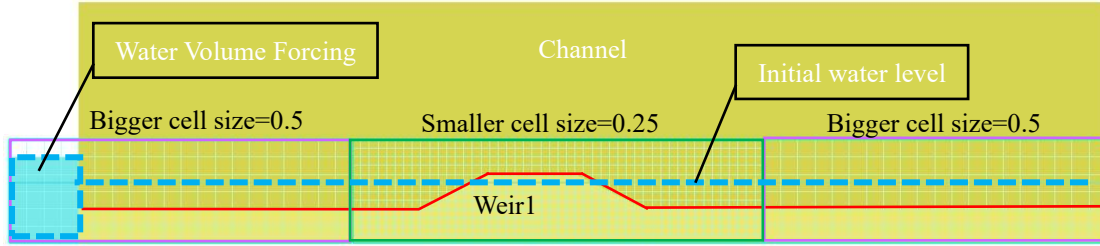


Fig. 6. Meshing in Y-Z Plane

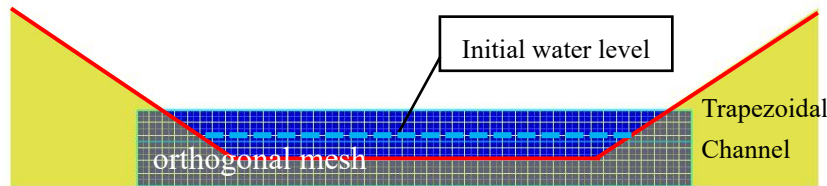


Fig. 7. Meshing in X-Z Plane

In terms of viscosity evaluation (turbulence module), the Renormalized group (RNG) model is employed to constrain the turbulent viscosity from being too high.

One location at the middle of weir at Y-Z plane is used to read the flow data including velocity and Fr.

## 3. Analysis and Discussion

### 3.1. Velocity distribution of the channel flow

Based on the currently known data, 14 locations in the channel are selected for discussion. From the MIKE software, the Fr in natural present condition ( $Fr_{pre}$ ) and the

Fr after optimisation ( $Fr_o$ ) are obtained from the water depth and flow velocity. The relevant data and flow profile are shown below.

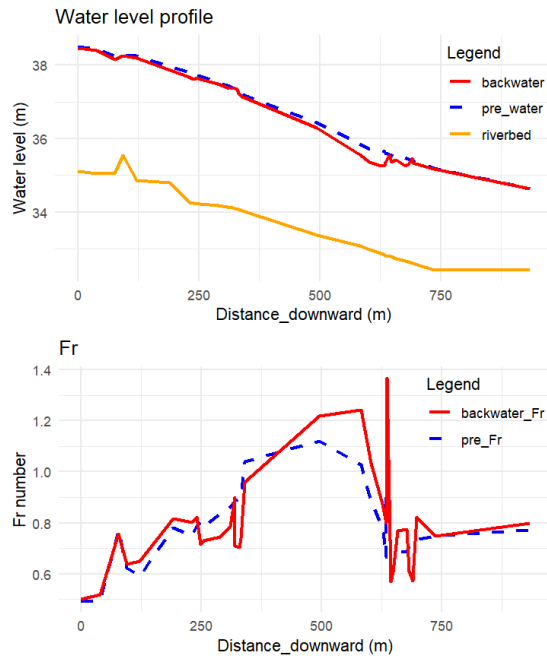


Fig. 8 Velocity and Fr profile

Distance	Fr <sub>pre</sub>	Fr <sub>o</sub>
0	0.39	0.64
76.45	0.41	0.93
93.95	0.53	0.54
122.05	0.63	0.78
191.05	1.27	0.9
230.05	1.14	1.15
320.05	0.95	1.33
406.45	1	0.83
453.04	1.37	0.99
494.72	1.17	1.01
581.71	1.14	1.33
633.73	0.87	0.88
736.43	0.77	0.96
844.05	0.83	1

Referring to the information about Shawan River, the diameter of the sand and gravel  $d=0.2$  mm, which resulted in a b-value of about 0.377 based on the results of JIA[4]. Use Equation(2-3) to calculate K:  $K = 4.49 \times 0.2^{-0.186} = 6.057$ .

From the design report, we get the average slope J value of the channel as 0.002. Based on simulation results, we get the velocity V at 14 locations in the natural state and calculate the average velocity  $V_{\text{mean}} = 1.86\text{m/s}$ .

Table. 3. Flow features form MIKE simulating results

Chainage	Slope J	V
0	0.002	0.911
76.45	0.002	0.993
93.95	0.002	1.03
122.05	0.002	0.946
191.05	0.002	2.573
230.05	0.002	1.64
320.05	0.002	2.525
406.45	0.002	1.933
453.04	0.002	2.255
494.72	0.002	2.105
581.71	0.002	2.435
633.73	0.002	2.33
736.43	0.002	2.043
844.05	0.002	2.304
Mean velocity		1.86

Therefore, the ideal  $Fr_{min}$  is obtained:  $Fr_{min\_s} = 6.057 \times (VJ)^{0.377} = 0.735$ .

By comparing the PUB\_COP\_7th\_Edition[7] in Singapore about the design  $Fr$ , we found that the value of  $Fr_{min\_s}$  is very close to the standard value of 0.8. In addition, according to the reference [4], the value of  $Fr_{min}$ , represents the highest stable condition of the channel. Therefore, combining the above two points, we believe that  $Fr_{min\_s}$  can be used as a standard value for the study area, which represents the most stable state of the river channel.

The optimisation effects will be analysed with respect to  $Fr_{min}$  according to the performance indicators.

The variance analysis is conducted in  $Fr_{min\_s}$ ,  $Fr_{pre}$  and  $Fr_o$ , with downstream flow direction is as following graph.

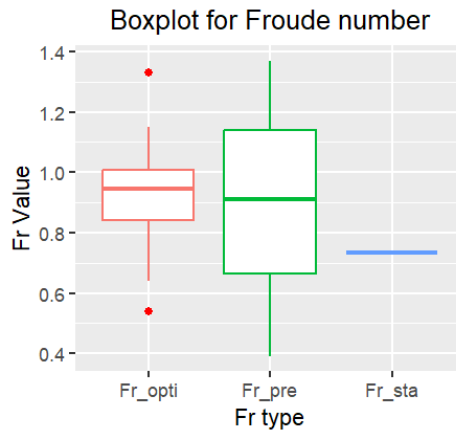


Fig. 9 Boxplot for Comparison of Fr

Upon analyzing the boxplot, we can see:

- 1) It is observed that the distribution trend of the  $Fr_o$  box is more concentrated. And 75% of the  $Fr_o$  are smaller than 1, showing a more stable flow condition and will not remain a long term supercritical flow.
- 2) The distribution trend of  $Fr_{pre}$  exhibits significant dispersion, with approximately 30% of the values exceeding 1, indicating highly unstable flow conditions.
- 3) The median of  $Fr_o$  is more variance of the stable index compared to  $Fr_{pre}$ , but the value is still close.

Therefore, from above statistical analysis, it can be concluded that the stability of optimization channel is better.

### 3.2. Submerged trapezoidal weir

We focus on submerged trapezoidal broad-crested weirs under various upstream face slopes and a long-term average water level of flow conditions. It is noted that the flow upstream of the weir is subcritical ( $Fr_1 < 1$ ), and then over the board weir crest the critical flow as transitional state occurs. Later, flow along the downstream weir face is supercritical ( $Fr_2 > 1$ ), and it shifts into subcritical flow at the downstream far away from the weir.

The results obtained from the simulations are presented below, showcasing the flow



properties by graphs and charts.

### 3.2.1. Flow surface profile

Use the computed free surface elevation to plot the streamline over these 3 kinds of weirs within a constant discharge. (See in Fig. 10). The transition about water profile at the downstream weir depends on the initial water level, so the relevant results at the downstream is not our theme.

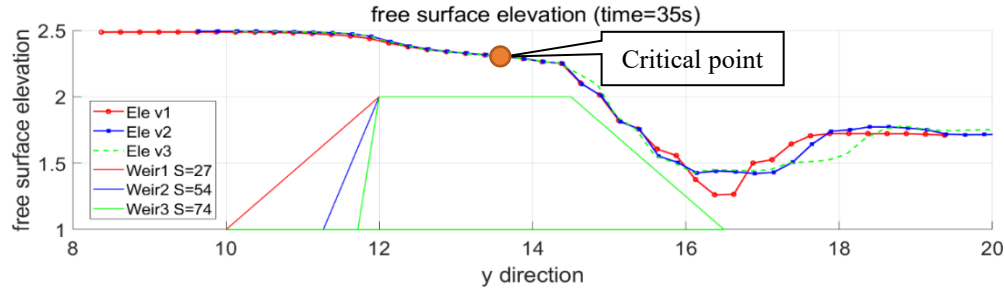


Fig. 10. computed water-surface profile over the weirs

- 1) In practice, undular flow leads to pressure redistributions and may damage the hydraulic structures, that must be avoided in the river engineering. It is illustrated in Fig. 10 that in this design of weir crest, the undular flow can be avoided. It can also be verified by the criterion for formation of undular flow [8]:

$$\frac{H_0 - Z}{L_{cr}} < 0.15 \quad (3-1)$$

where numerator is the upstream head above on the weir crest, and the weir crest length  $L_{cr}=2.5m$ . In this case,  $\frac{H_0 - Z}{L_{cr}} = 0.2 < 0.5$ , that means the flow form over the weir is usually a parallel streamline. Specifically, for a steep slope, the water profile becomes smoother and flatter.

- 2) As can be seen, with the increasing slope  $\theta$ , the hydraulic jump at the downstream is shifted far away from the weir heel.

### 3.2.2. Critical point

It is obvious for a weir controlling the discharge to convert the flow along the weir to be supercritical (See in Fig. 11).

The first transition to the critical flow takes place on the crest, and upstream slope almost do not change the critical location. And then  $Fr$  reaches its peak close to the weir heel. Combination with the water profile, higher  $Fr$  in Weir2 indicates the faster velocity and lower water depth, that may cause more erosion damage.

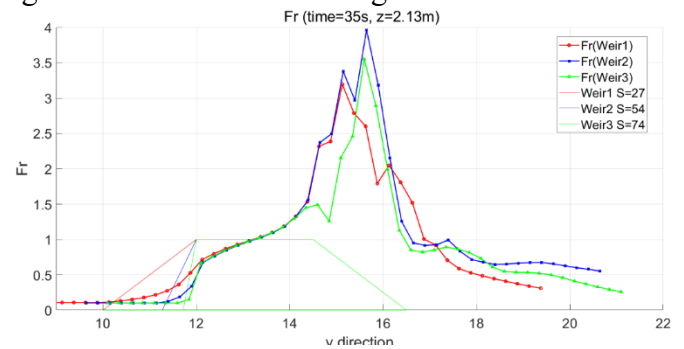


Fig. 11. Froude number along the stream

### 3.2.3. Velocity distribution

Fig. 13 shows the velocity distribution with color by 3D velocity magnitude. And the maximum vertical velocity is extracted in Table. 4.

The total velocity distribution along the streamline can be described as following:

- 1) At the upstream of the weirs, the velocity profiles are straight and uniform.

- 2) The flow accelerates gradually when it reaches the weirs. Compared with these mild upstream slopes, a steep slope causes a sharp increasing velocity at the corner of the weir. Because of steep slopes or shallow water depths, the flow behind the weir tends to slow significantly and the water accumulates behind the weir, that implies that the discharge over the weir reduces. Since the discharge for submerged trapezoidal weirs in open channel can be obtained by:

$$Q = C_D B \sqrt{2gH}$$

where  $H$  is total overflow head, it can be illustrated that the steep slopes reduce the discharge coefficient  $C_D$ . [9]

- 3) At the downstream of the weirs, the maximum of vertical velocity usually appears close to the weir heel. Although the mild slope leads to the relatively lower averaged velocity magnitude, it causes an obviously great vertical velocity. it is noted that the steep slope leads to a minimum vertical velocity and relatively lower averaged velocity magnitude.

Table. 4 Maximum vertical velocity along downstream face of weir

Weir	Max w (m/s)	Distance to heel(m)
1	2.12	0.625
2	1.91	1.855
3	1.40	1.655

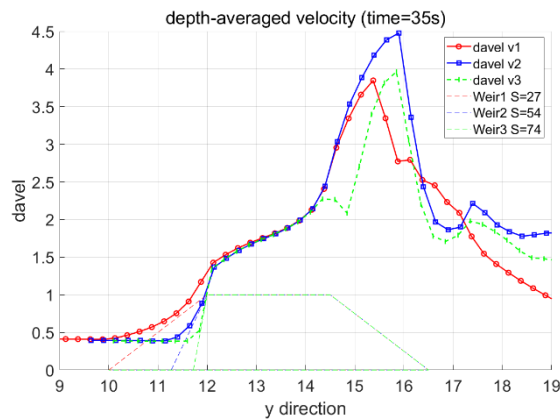


Fig. 12. Depth-averaged velocity (unit: m/s)

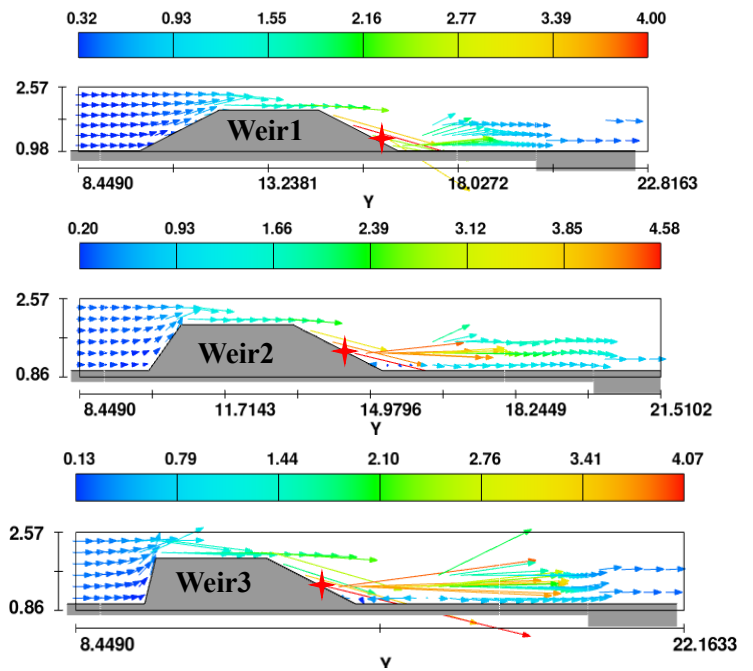


Fig. 13 Velocity distribution

- 4) Compare the flow velocity profile before and after weir in Fig. 14, where the downstream measurement distance is 2m from the heel. In the velocity profile after the weir 3, a sudden change was observed.

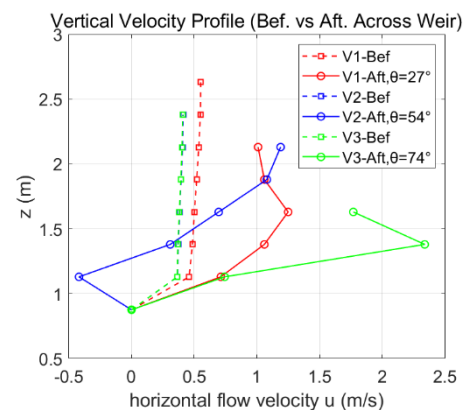


Fig. 14 Comparison of flow velocity profile before and after weir



### 3.2.4. Turbulence Intensity

Turbulence usually occur before and after weirs and can cause energy losses, noise and structural vibrations. The better shape of weirs is designed to reduce or avoid these phenomena.

We use the turbulence intensity  $I$  to evaluate the turbulence after weirs:

$$I = \sqrt{\frac{k_T}{\bar{K}}} \quad (3-2)$$

where  $k_T$  is the turbulent kinetic energy,  $\bar{K}$  is the mass-averaged mean kinetic energy in the domain. [6]

As can be seen, that the distinct range turbulence with the similar intensity occurs at the downstream of weirs, and Weir3 with a steep slope form a smaller range turbulence.

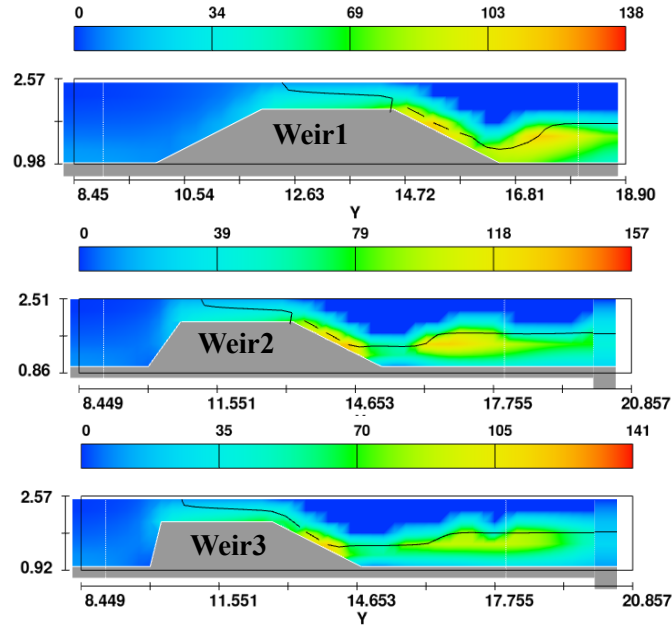


Fig. 15. Turbulence Intensity (unit: %)

### 3.2.5. Sediment transport

It is known that the total sediment discharge = suspended load + bed load, and the main component of the sediment in Shawan Channel is sand with  $d=0.2mm$ .

#### 1) Bed-load

A common and useful approach to the quantification of bedload transport is to empirically relate the non-dimensional Einstein number,  $q_b^*$ . [10] One of the popular bedload transport relations for well-sorted sediments by Engelund and Fredsoe:

$$q_b^* = 18.74(\tau^* - \tau_c^*)(\tau^{*0.5} - 0.7\tau_c^{*0.5}), \quad \tau_c^* = 0.05 \quad (3-3)$$

Shields stress: 
$$\tau^* = \frac{\tau_b}{\rho R g D} \quad (3-4)$$

Shear stress with Chezy coefficient: 
$$\tau_b = \frac{\rho g}{c^2} V^2 \quad (3-5)$$

where  $V$  is the magnitude of flow velocity. As a minimum vertical velocity and relatively lower averaged velocity magnitude in Weir3, that implies a steep upstream slope can reduce the sediment transport or even erosion, to some extents.

#### 2) Simple analysis without considering the effect on water depth

The Hjulström-Sundborg diagram shows the likelihood of a grain being eroded, transported, or deposited but it does not take the water depth into account.

As the sand diameter in Shawan River is around  $D=0.2\text{mm}$ , and the velocity at the downstream of the weir is great than  $1\text{m/s}$ , it is highly possible to occur erosion.

It should be noted that sedimentation is caused by flow velocity deceleration and erosion is caused by flow acceleration, that is ignored in Hjulström curves.

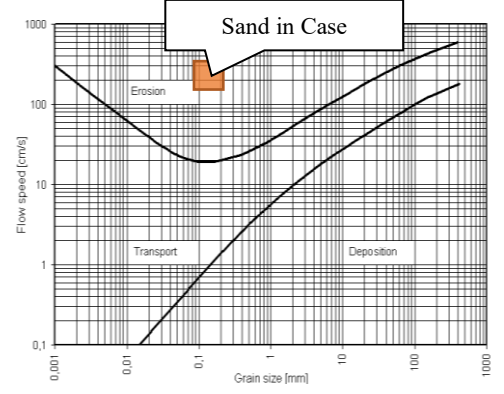


Fig. 16. Hjulström-Sundborg diagram

### 3) Shear stress and suspension sediment in SRD

Apply the effective shields parameter  $\theta'$  and the particle Reynolds number  $Rp$  in the Shields regime diagram (SRD) to define the suspension concentration and condition above the bedform.

For nature fine particles sediment, we determine a critical parameter in the SRD, the particle Reynolds number  $Rp$ , explicitly using the following formula [11]:

$$Rp = \frac{Re}{\sqrt{\theta}} = \frac{\sqrt{(s-1)gd}d}{\nu}$$

where  $Rp$  depends (among other things) on the sediment size  $d$ , but not other hydro-dynamic factors.

Then, the dimensionless Shields parameter can be obtained:

$$\theta = \frac{Uf^2}{(s-1)gd}$$

For the effective Shields parameter  $\theta'$ , the implicit solution and statement is required:

- 1) For the upper regime ( $\theta' > 0.55$ ):
- 2) For the lower regime ( $\theta' \leq 0.55$ ):

$$\theta' = [0.702\theta^{-1.8} + 0.298]^{-1/1.8}$$

$$\theta' = 0.06 + 0.3\theta^{3/2}$$

Therefore, we can predict bedform type in the Shields regime diagram in terms of the particle Reynolds number in the following graph.

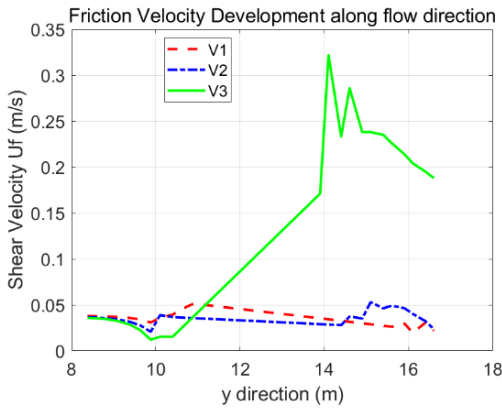


Fig. 17 Shear stress

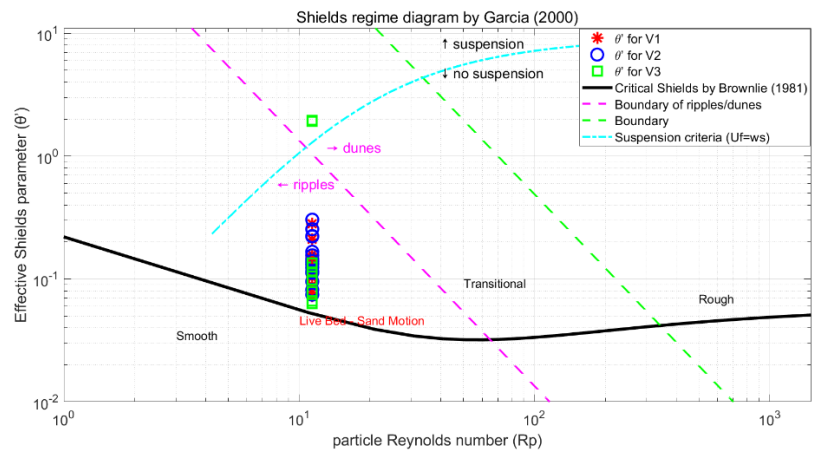


Fig. 18 SRD

We can see that a steep upstream slope in weir 3 leads a significant velocity change and

locally higher shear stress, facilitating more suspension and reducing sedimentation.

## 4. Conclusion

### 4.1. Optimization channel

- 1) In the condition of long-term averaged discharge and water level, the peak value relative error  $\sigma$  for optimised channel is lower and its stability is better.
- 2) In the condition of 100-year return period storm, the correlation coefficient for optimised channel is higher and higher than 0.8. The optimization channel performs better than the natural situation in extreme condition.

### 4.2. Suitable Shape of the Trapezoidal-Board weir

According to the comparison of weirs in terms of the flow state and sedimentation in Table. 5, the conclusion are following:

- 1) In the design of weir crest, the undular flow can be avoided.
- 2) Flow over the weir is usually a parallel streamline.
- 3) Considering a larger flow capacity of weir, a mild upstream slope at the upstream is better.
- 4) A steeper upstream slope may causes a higher shear stress in the downstream close to the heel, that highly increases the likelihood of erosion occurring downstream.
- 5) In terms of the flow stability, a steep slope at the upstream shows a positive effect.

Table. 5 Analysis of 3 types weir

Weir	Flow Condition	Velocity distribution	Turbulence	Sediment transport
1 $\theta=27^\circ$ mild	1) No undular flow; 2) A parallel streamline.	1) Relatively lower averaged velocity magnitude; 2) Obviously great vertical velocity may damage the hydraulic structures.	Biggest range of turbulence	Stable sheart stress and reduce the suspension sediment transport.
2 $\theta=54^\circ$	Too high value of $Fr$	-	-	
3 $\theta=74^\circ$ steep	1) Water profile becomes smoother and flatter; 2) Hydraulic jump at the downstream is shifted far away from the weir heel.	1) Reduces the discharge coefficient $C_D$ ; 2) Leads to a minimum vertical velocity and relatively low averaged velocity magnitude.	Smallest range of turbulence	Highly possible to occur erosion in downstream as highr shear stress.

## References

- [1] S. E. Greco and E. W. Larsen, 'Ecological design of multifunctional open channels for flood control and conservation planning', *Landscape and Urban Planning*, vol. 131, pp. 14–26, Nov. 2014, doi: 10.1016/j.landurbplan.2014.07.002.
- [2] Shenzhen Water Bureau, "Preliminary Design Report on River Training in Shawan River Basin of Shenzhen", Sep, 2015.
- [3] MIKE 11 User Manual.
- [4] Y. Jia, 'Minimum froude number and the equilibrium of alluvial sand rivers', *Earth Surf. Process. Landforms*, vol. 15, no. 3, pp. 199–209, May 1990, doi: 10.1002/esp.3290150303.
- [5] M. R. Madadi, A. Hosseinzadeh Dalir, and D. Farsadizadeh, 'Investigation of flow characteristics above trapezoidal broad-crested weirs', *Flow Measurement and Instrumentation*, vol. 38, pp. 139–148, Aug. 2014, doi: 10.1016/j.flowmeasinst.2014.05.014.
- [6] FLOW-3D, 2012. FLOW-3D User Manual. Flow Science Inc.
- [7] 'PUB\_COP\_7th\_Edition in Singapore.pdf'. Accessed: Oct. 09, 2023. [Online]. Available: [https://www.pub.gov.sg/Documents/PUB\\_COP\\_7th\\_Edition.pdf](https://www.pub.gov.sg/Documents/PUB_COP_7th_Edition.pdf)
- [8] O. Castro-Orgaz and H. Chanson, 'Near-critical free-surface flows: real fluid flow analysis', *Environ Fluid Mech*, vol. 11, no. 5, pp. 499–516, Oct. 2011, doi: 10.1007/s10652-010-9192-x.
- [9] H. M. Fritz and W. H. Hager, 'Hydraulics of Embankment Weirs', *Journal of Hydraulic Engineering*, vol. 124, no. 9, pp. 963–971, Sep. 1998, doi: 10.1061/(ASCE)0733-9429(1998)124:9(963).
- [10] M. H. Chaudhry, *Open-Channel Flow*. Cham: Springer International Publishing, 2022. doi: 10.1007/978-3-030-96447-4.
- [11] R. A. Gaines and R. H. Smith, 'Micro-Scale Loose-Bed Physical Models', in *Hydraulic Measurements and Experimental Methods 2002*, Estes Park, Colorado, United States: American Society of Civil Engineers, Oct. 2002, pp. 1–12. doi: 10.1061/40655(2002)78.